Jpn. J. Appl. Phys. Vol. 37 (1998) pp. 584–588
Part 1, No. 2, February 1998

Electron Energy-Loss Spectroscopy Study of the Metal-Insulator Transition in V_2O_3

Hiroyuki ABE, Masami TERAUCHI, Michiyoshi TANAKA and Shik SHIN[1]
Research Institute for Scientific Measurements, Tohoku University, Sendai 980-77, Japan
[1]*Synchrotron Radiation Laboratory, Institute for Solid State Physics, The University of Tokyo, Tokyo 188, Japan*

(Received July 28,1997; accepted for publication November 17,1997)

Electron energy-loss spectra of V_2O_3 of the paramagnetic metallic (PM) and antiferromagnetic insulating (AFI) phases have been measured by a high-resolution transmission electron energy-loss spectroscopy (EELS) technique. An excitation at about 1 eV was previously observed in both the PM and AFI phases by an optical measurement and assigned to the excitation of a free-carrier plasmon. A sharp peak has, however, been observed at 1.1 eV in our EELS spectra of the PM phase but not in those of the AFI phase. We assigned the peak to an interband plasmon due to d-d transitions by inspecting the dielectric function derived from the EELS spectra. The peak of the O $1s$ EELS spectra due to the O $1s \rightarrow$ V $3d(t_{2g})$ transition increased in energy by 0.4 eV but decreased in intensity at the transition from the PM phase to the AFI phase. The increase of the energy is due to a splitting of the V $3d(t_{2g})$ band, which is partly filled at the PM phase, into the fully occupied and unoccupied bands and a shift of the unoccupied band to an energy higher than the Fermi level in the PM phase. The decrease of intensity is considered to be due to the decrease of the transition probability of the O $1s \rightarrow$ V $3d(t_{2g})$ transition, which is attributed to the decrease of the hybridization of the V $3d$ with O $2p$ orbitals at the transition from the PM phase to the AFI phase.

KEYWORDS: metal-insulator transition, EELS, free-carrier plasmon, interband transition, interband plasmon, unoccupied density of states

1. Introduction

In a previous study, we showed a change in the electronic structure of VO_2 at the metal-insulator transition (MIT) using the high-resolution transmission electron energy-loss spectroscopy (EELS) technique.[1)] A sharp peak was observed at 1.2 eV in the EELS spectra of the metallic phase but not in those of the insulating phase. An excitation at about 1 eV had been observed by an optical measurement and assigned to the excitation of a free-carrier plasmon.[2)] We, however, assigned the peak to an interband transition or a d–d transition from the inspection of the dielectric function derived from the loss function with the help of an energy band diagram previously given.[3)] The peak due to the O $1s \rightarrow$ V $3d(t_{2g})$ transition in the O $1s$ EELS spectra decreased in intensity but increased to full width at half-maximum (FWHM) at the transition from the metallic phase to the insulating phase. These changes were interpreted by changes of the band structure. That is, the $d_{\|}$ band splits into the upper unoccupied and lower occupied $d_{\|}$ bands and the upper $d_{\|}$ band rises above the π^* band in the insulating phase, but the $d_{\|}$ band is unsplit and located within the π^* band in the metallic phase.[1)]

Vanadium sesquioxide (V_2O_3) also undergoes the MIT with a change of temperature,[4)] which is accompanied by changes of the crystal[5)] and magnetic[6)] structures. It has the corundum structure with space group $R\bar{3}c$ in the paramagnetic metallic (PM) phase above 165 K and a monoclinic structure with space group $B2/b$ in the antiferromagnetic insulating (AFI) phase below 165 K. Changes in the electronic structure of V_2O_3 at the MIT were studied by optical spectroscopy[7–10)] and photoemission spectroscopy (PES).[10–17)] Stizza *et al.*[8)] measured the thermoreflectance spectra of V_2O_3 at the PM and AFI phases, and observed a negative peak at about 1 eV in both phases. They identified the peak to be due to a free-carrier plasmon as in the case of the metallic phase in VO_2.[2)] The peak energy increased by 0.14 eV with a decrease in temperature from 285 to 122 K. Since free carriers do not exist in the insulator or the AFI phase, the negative peak should not be due to the free-carrier plasmon. We considered that the reexamination of the excitation at about 1eV observed in the thermoreflectance spectra[8)] is necessary. A similar assignment to that for VO_2 given by us[1)] may also be possible in V_2O_3. It is noted that good quality specimens without oxygen deficiencies should be examined to allow detailed discussion on the change in intrinsic electronic structures of V_2O_3 at the MIT because oxygen deficiencies introduce free carriers.

Abbate *et al.*[18)] measured the V $2p$ and O $1s$ spectra of V_2O_3 at the PM phase by X-ray absorption spectroscopy with an energy resolution of 0.15 eV. Lin *et al.*[19)] also measured those spectra by a transmission EELS with an energy resolution of 0.5 eV. The V $2p$ spectrum measured by Abbate *et al.*[18)] is almost consistent with that measured by Lin *et al.*,[19)] although fine structures are seen in the spectrum of Abbate *et al.*[18)] but not in that of Lin *et al.*[19)] The peak intensity of the O $1s \rightarrow$ V $3d(t_{2g})$ transition is nearly the same as that of the O $1s \rightarrow$ V $3d(e_g)$ transition in the O $1s$ spectrum measured by Abbate *et al.*,[18)] while the former is smaller than the latter in the O $1s$ spectrum measured by Lin *et al.*[19)] The change of the unoccupied density of states (DOS) of the V $3d$ band due to the MIT can be seen directly from the change of the O $1s$ spectra. However, since Abbate *et al.*[18)] and Lin *et al.*[19)] did not measure the spectra at the AFI phase, the change of the unoccupied DOS of the V $3d$ band was left unknown.

We have measured EELS spectra at valence and core electron excitation regions from perfect single crystalline areas of V_2O_3 using the high-resolution transmission EELS microscope to reveal the change in electronic structures at the MIT.

2. Experimental

The high-resolution EELS microscope used was developed as a project of Joint Research with Industry by the Ministry of Education, Science, Sports and Culture, Japan.[20,21)] The EELS microscope is equipped with a thermal-type field emission gun as the electron source and specially designed double-focus Wien filters as the monochromator and the analyzer. The EELS microscope incorporates an illumination lens system, a specimen goniometer and an imaging lens system of a

JEM1200EX transmission electron microscope. EELS spectra were taken by a parallel-recording system using a charge-coupled device (CCD) camera. The best values at present of the full width at half-maximum (FWHM) of the zero-loss peak are 15 meV without a specimen and 25 meV with a specimen. The incident electron energy was set at 60 keV. The retarding potential of the monochromator was set to be 51 V and that of the analyzer at 200–520 V in this experiment.

Specimens for electron energy-loss spectra were prepared by crushing single crystals and placing the fragments on mesh for electron microscopy. Electron energy-loss spectra were obtained from specimen areas of 180 nm diameter. The specimen areas were judged to be perfectly crystalline from their good electron diffraction patterns. The specimens were cooled in a cooling holder for electron microscopy. The temperature of the specimens was measured by a thermocouple near the specimens. The apparent temperature of the transition into the PM phase was 140 K, against a reported value of 165 K.[4)]

3. Results and Discussion

3.1 EELS spectra of the valence electron excitation region

Figure 1 shows EELS spectra of V_2O_3 measured at the AFI (100 K) and PM (140 and 300 K) phases over an energy range of 0–60 eV with energy resolutions of 0.13 and 0.14 eV for the FWHM of the zero-loss peak, respectively. The small peak at about 5 eV is assigned to the interband transition from the O 2*p* band to the V 3*d* band.[10)] The sharp peak at about 12 eV is attributed to the interband plasmon due to the transition from the O 2*p* band to the V 3*d* band.[10)] The peak at about 17 eV is assigned to the interband transition from the O 2*p* band to the V 4*s*,4*p* band.[10)] The large peak at about 27 eV is due to the collective excitation of all valence electrons (valence plasmon). The calculated plasmon energy using the Drude model is about 20 eV. This value does not agree with the experimental one. The plasmon energy ($\hbar\omega_p$), however, is calculated more accurately by the Lorentz model using the following equation

$$\hbar\omega_p = \sqrt{(\hbar\omega_p^{(f)})^2 + (\hbar\omega_0)^2}, \tag{3.1}$$

where $\hbar\omega_p^{(f)}$ is the plasmon energy calculated from the Drude model and $\hbar\omega_0$ is the interband transition energy. By substituting $\hbar\omega_p^{(f)} = 20$ eV and $\hbar\omega_0 = 17$ eV, which is the closest interband transition energy to the valence plasmon energy, into eq. (3.1), we obtain $\hbar\omega_p = 26$ eV, which agrees well with the experimental value of 27 eV. The peak at about 43 eV and the shoulder at about 48 eV are assigned to the transitions from the V 3*p* core levels to the V 3*d* band by referring to X-ray PES (XPES) spectra.[16)] The broad peak at about 52 eV is attributed to the double loss of the valence plasmon.

Figure 2 shows the EELS spectra of V_2O_3 measured at the AFI (100 and 130 K) and PM (140 and 300 K) phases over an energy range of 0–10 eV with energy resolutions of 100 and 90 meV for the FWHM of the zero-loss peak, respectively. The peak at 1.1 eV indicated by an arrow, and the shoulder at about 1.7 eV indicated by a vertical line, appear upon the transition into the PM phase (140 K). This peak may correspond to that observed at 0.93 eV in the thermoreflectance spectra measured at 144 K by Stizza *et al.*[8)] They assigned the peak as the free-carrier plasmon peak, although the peak was also

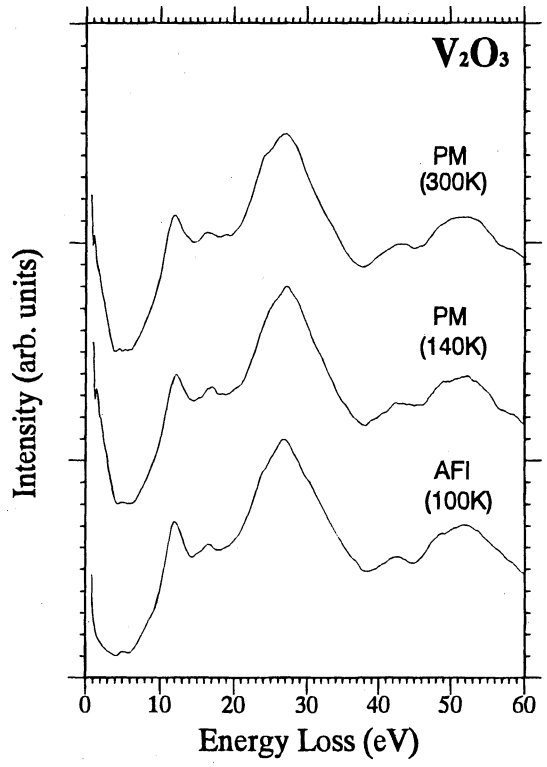

Fig. 1. Valence electron excitation spectra of V_2O_3 measured at the AFI (100 K) and PM (140 and 300 K) phases over an energy range of 0–60 eV with energy resolutions of 0.13 and 0.14 eV, respectively.

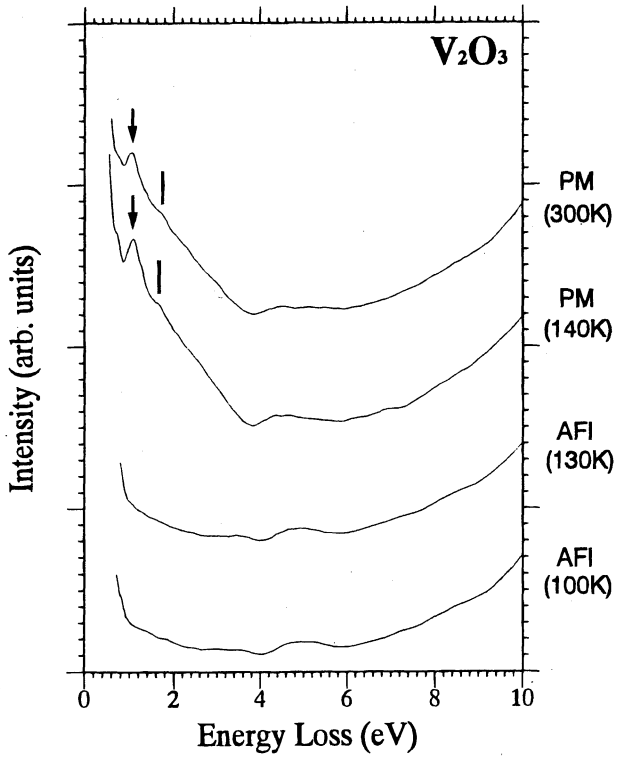

Fig. 2. Valence electron excitation spectra of V_2O_3 measured at the AFI (100 and 130 K) and PM (140 and 300 K) phases over an energy range of 0–10 eV with energy resolutions of 100 and 90 meV, respectively. The peak at 1.1 eV indicated by an arrow and the shoulder at 1.7 eV indicated by a vertical line appear upon the transition into the PM phase (140 K).

observed at the AFI phase. We, however, observed the peak at about 1 eV only at the PM phase but not at the AFI phase. The peak energy in the PM phase did not change with increasing temperature from 140 to 300 K, whereas Stizza *et al.*[8] observed a decrease of its energy by 0.14 eV by increasing the temperature from 122 (AFI phase) to 285 K (PM phase).

The upper panels of Figs. 3(a) and 3(b) show the loss function ($\mathrm{Im}[-1/\varepsilon(\omega)]$) of the AFI (100 K) and PM (140 K) phases, respectively, derived from Figs. 1 and 2. The contributions of the direct beam and multiple scattering were removed by a Lorentz fit and the Fourier-log deconvolution method,[22] respectively. The absolute value of the loss function at the PM phase was determined by applying $\mathrm{Re}[-1/\varepsilon(0)] = 0$. Since the refractive index of the AFI phase is not known, the absolute value of the loss function of the AFI phase was determined using the sum rule

$$\int_0^\infty \omega\, \mathrm{Im}\left[-\frac{1}{\varepsilon(\omega)}\right] d\omega = \frac{\pi}{2}(\omega_\mathrm{p}^{(f)})^2, \qquad (3.2)$$

$$\omega_\mathrm{p}^{(f)} = (Ne^2/\epsilon_0 m)^{1/2}, \qquad (3.3)$$

where ϵ_0 is the dielectric permittivity of vacuum, N is the density of electrons, e is the electron charge and m is the mass of an electron. The dielectric function was calculated from the loss function and $\mathrm{Re}[1/\varepsilon(\omega)]$, which was derived from the loss function by Kramers-Kronig analysis. The integration with energy was carried out up to 400 eV in Fourier-log deconvolution, determination of the absolute value of the loss function and in Kramers-Kronig analysis, where the loss function above 60 eV was obtained by extrapolating the loss function using E^{-4} dependence.[1,23] The value of $\hbar\omega_\mathrm{p}^{(f)}$ was taken to be 31.9 eV, which was calculated by eq. (3.3) using the number of electrons contributing to the excitation below 60 eV. The lower panels of Figs. 3(a) and 3(b) show the real (ε_1) and imaginary (ε_2) parts of the dielectric function of the AFI (100 K) and PM (140 K) phases, respectively. The condition for the plasmon excitation ($\varepsilon_1 = 0$) is not satisfied at about 1 eV in the AFI phase (100 K) [Fig. 3(a)]. Therefore, it is clear that the free-carrier plasmon excitation does not exist in the AFI phase.

On the other hand, the condition for the plasmon excitation ($\varepsilon_1 = 0$) is satisfied at 1.0 eV in the PM phase (140 K) [Fig. 3(b)]. Thus, a peak at 1.1 eV in the loss function of the PM phase is assigned to a plasmon excitation. The free-carrier plasmon is expected to be observed at 7.3 eV, which is calculated from eq. (3.3) using carrier density at the PM phase of $3.85 \times 10^{28}\,\mathrm{m}^{-3}$.[24] Thus, the peak at 1.1 eV is not assigned to the free-carrier plasmon excitation. It is considered that interband transitions shift the plasmon energy from the calculated value of 7.3 eV to 1.1 eV as in the case of interband plasmon excitations in Ag and Cu,[25] which originate from the interaction between the plasmon and the interband transitions. Actually it is plausible that the peak at 1.1 eV in the loss function is assigned to an interband plasmon peak because ε_1 is equal to zero (plasmon character) at 1.1 eV and ε_2 shows peaks and shoulders (interband transition character) around 1.1 eV. The excitation at about 1eV observed by Stizza *et al.*[8] should be the interband plasmon excitation. Balberg[26] reported that the minimum transition energy from the O 2*p*

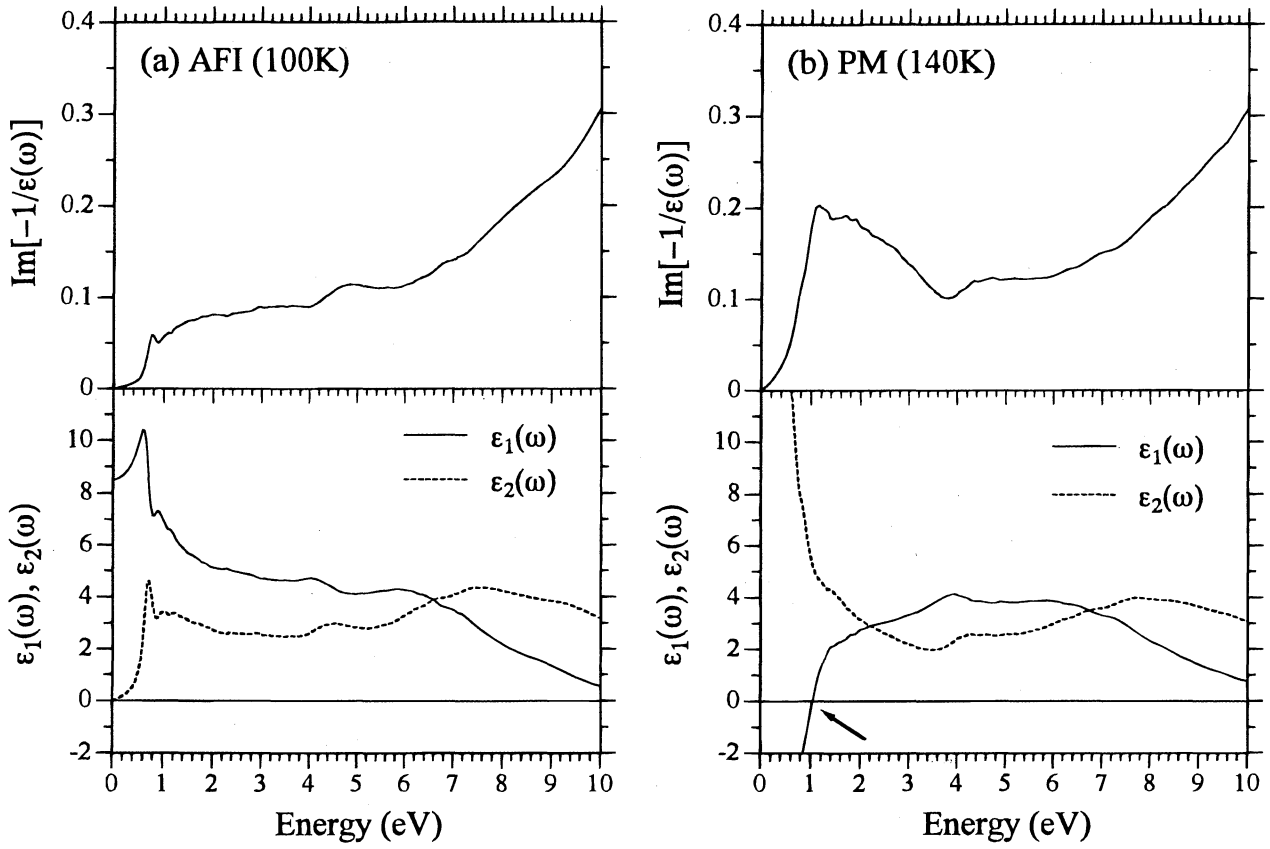

Fig. 3. The loss function ($\mathrm{Im}[-1/\varepsilon(\omega)]$), the real part ($\varepsilon_1$) and the imaginary part (ε_2) of the dielectric function of V_2O_3 at the AFI phase (100 K) (a) and the PM phase (140 K) (b). The dielectric function was derived by Kramers-Kronig analysis of the loss function.

band to the unoccupied V $3d$ band is 3.5 eV and that from the occupied V $3d$ band to the V $4s$,$4p$ band is greater than 2.6 eV. Thus, peaks and shoulders below 2.6 eV in the loss function cannot be assigned to these transitions. The peaks and shoulders must be due to d–d transitions. Therefore, the interband transitions that shift the plasmon energy are mainly the d–d transitions. The transitions are allowed, although they are formally forbidden by the dipole selection rule, because the V $3d$ band has a p-like characteristic due to the overlap of the V $3d$ orbitals with the O $2p$ orbitals. Since the average V–O distance, which is obtained by averaging the six V–O distances in the VO_6 octahedron, slightly decreased at the transition from the AFI phase to the PM phase,[5] the hybridization of the V $3d$ with O $2p$ orbitals is stronger in the PM phase than in the AFI phase. Thus, the d–d transitions are expected to be stronger in the PM phase than in the AFI phase. We conclude that the peak at 1.1 eV in the loss function is not due to the free-carrier plasmon excitation but is due to the interband plasmon excitation, the interband transition being the d–d transitions which are enhanced in the PM phase.

3.2 *EELS spectra of the core electron excitation region*

Figure 4 shows EELS spectra measured at the AFI (100 K) and PM (300 K) phases over an energy range of 507–543 eV with an energy resolution of 0.21 eV for the FWHM of the zero-loss peak. The spectra below 527 eV are the V $2p$ EELS spectra and those above 527 eV are the O $1s$ EELS spectra. The peaks at about 516 and 522 eV are attributed to excitations from the V $2p_{3/2}$ and V $2p_{1/2}$ core levels, respectively. The peak energy of the V $2p$ EELS spectrum hardly changed at the transition from the PM phase to the AFI phase. The shoulders at 512.1 and 519.4 eV, indicated by arrows in the spectrum of the PM phase, however, changed into peaks as a result of the transition to the AFI phase. The experimental spectral intensity ratio of the V $2p_{3/2}$ to V $2p_{1/2}$ excitations is different from that expected from the spin-orbit splitting (2 : 1). This is because a strong core-hole interaction exists between the hole in the V $2p$ core level and the electron excited into the unoccupied V $3d$ band from the core level.[27] Theoretical calculations are needed to quantitatively explain the V $2p$ EELS spectra.

On the other hand, the core-hole interaction between the hole in the O $1s$ core level and the electron excited into the unoccupied V $3d$ band from the core level is not strong because the overlap of the O $1s$ orbital with the V $3d$ orbitals is small compared with that of the V $2p$ orbitals with the V $3d$ orbitals. Thus, the change of the unoccupied V $3d$ band at the MIT can be directly related to the change of the O $1s$ EELS spectra. The peaks at about 529 and 532 eV are assigned to the transitions from the O $1s$ core level to the unoccupied V $3d(t_{2g})$ and V $3d(e_g)$ bands, respectively. These transitions are possible through the admixture of the V $3d$ orbitals with the O $2p$ orbitals, although they are not allowed as a dipole transition. The broad peak at about 542 eV is assigned to the transition from the O $1s$ core level to the V $4s$,$4p$ band. The peak (t_{2g} peak) due to the O $1s \rightarrow$ V $3d(t_{2g})$ transition increased in energy by 0.4 eV but decreased in intensity at the transition from the PM phase to the AFI phase. The increase of energy is due to a splitting of the V $3d(t_{2g})$ band, which is partly filled at the PM phase, into the fully occupied and unoccupied bands and a shift of the unoccupied band to an energy higher than the Fermi level in the PM phase. The decrease of the intensity is considered to be due to the decrease of the transition probability of the O $1s \rightarrow$ V $3d(t_{2g})$ transition, which is attributed to the decrease of the hybridization of the V $3d$ with O $2p$ orbitals at the transition. The peak (e_g peak) due to the O $1s \rightarrow$ V $3d(e_g)$ transition consists of two close peaks, resulting in a trapezoid shape. The peak of a lower energy shifted to a high energy by 0.3 eV, but that of a higher energy hardly shifted at the transition. We revealed the change of the unoccupied DOS of the V $3d$ band from the change of the t_{2g} and e_g peaks at the MIT.

Figure 5 shows a combination of our O $1s$ EELS spectra

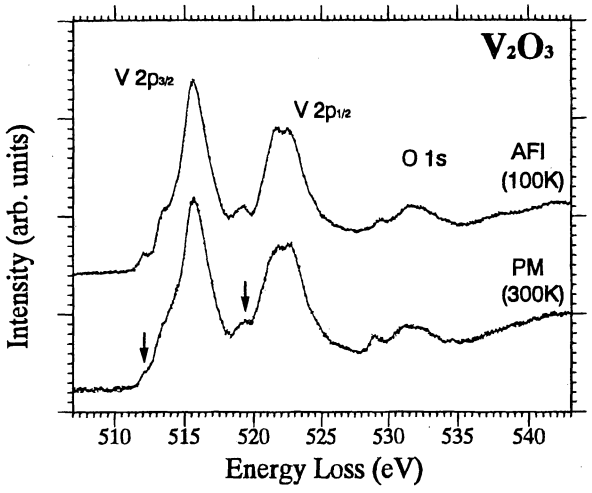

Fig. 4. V $2p$ and O $1s$ core electron excitation spectra of V_2O_3 measured at the AFI (100 K) and PM (300 K) phases over an energy range of 507–543 eV with an energy resolution of 0.21 eV.

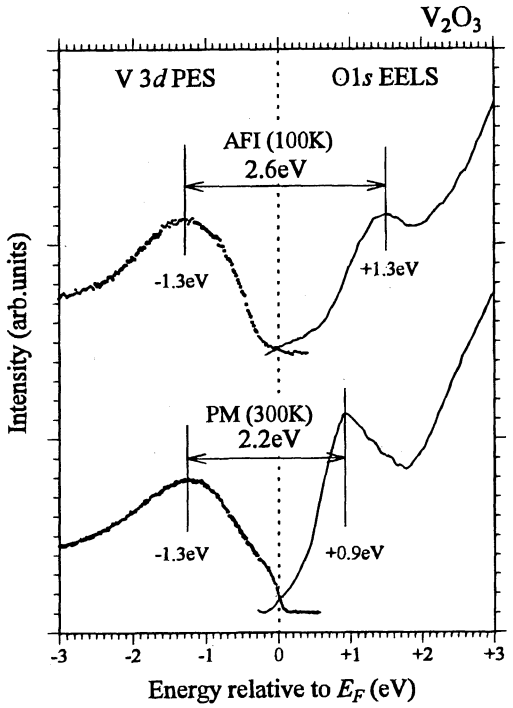

Fig. 5. O $1s$ core electron excitation (line) and photoemission (dot) spectra of V_2O_3. These spectra are aligned at the Fermi level. Photoemission spectra are refered from ref. 17.

and the PES spectra of Shin *et al.*,[17] which are aligned at the Fermi level. The energy position of the Fermi level of the O 1*s* EELS spectra of the PM phase was assigned to the position of a sharp rise (the Fermi edge) at the onset. We assumed that the energy of the Fermi level in the AFI phase is the same as that in the PM phase. It is clearly seen in the figure that the peak energy of the O 1*s* EELS spectra increase by 0.4 eV but that of the PES spectra do not change at the transition from the PM phase to the AFI phase. Since peaks of the PES and inverse PES (IPES) spectra respectively correspond to the lower and upper Hubbard bands in the $4f$ electron system, the energy difference between these peaks expresses a Hubbard U between $4f$ electrons. The energy difference in the case of the $3d$ electron system should be considered to be an effective Hubbard U (U_{eff}) because $3d$ electrons do not strongly localize like $4f$ electrons. Unfortunately, the IPES spectra have never been measured, whereas the PES spectra of V_2O_3 were measured by several investigators.[10–15,17] Using the O 1*s* EELS spectra in place of the IPES spectra, the energy difference between the peaks was measured as about 2.2 and 2.6 eV at the PM and AFI phases (Fig. 5), respectively. When an XPES study of an oxide superconductor $(La_{1-x}Sr_x)_2CuO_4$[28] is referred to, in which the U_{eff} between Cu $3d$ electrons did not change at the MIT, the energy difference between the peaks in Fig. 5 is less likely to be assigned to the change in U_{eff} between V $3d$ electrons. The energy difference may be due to the difference of the overlapping of V $3d$ orbitals with O $2p$ orbitals between the AFI and PM phases.

Acknowledgements

The authors would like to thank Mr. F. Sato for his skillful technical assistance. The present work was partly supported by a Grant-in-Aid from the Ministry of Education, Science, Sports and Culture.

1) H. Abe, M. Terauchi, M. Tanaka, S. Shin and Y. Ueda: Jpn. J. Appl. Phys. **36** (1997) 165.
2) A. Bianconi, S. Stizza and R. Bernardini: Phys. Rev. B **24** (1981) 4406.
3) E. Caruthers, L. Kleinman and H. I. Zhang: Phys. Rev. B **7** (1973) 3753.
4) F. J. Morin: Phys. Rev. Lett. **3** (1959) 34.
5) P. D. Dernier and M. Marezio: Phys. Rev. B **2** (1970) 3771.
6) R. M. Moon: Phys. Rev. Lett. **25** (1970) 527.
7) A. S. Barker Jr. and J. P. Remeika: Solid State Commun. **8** (1970) 1521.
8) S. Stizza, I. Davoli, R. Bernardini, A. Bianconi and M. Benfatto: Solid State Commun. **48** (1983) 471.
9) G. A. Thomas, D. H. Rapkine, S. A. Carter, A. J. Mills, T. F. Rosenbaum, P. Metcalf and J. M. Honig: Phys. Rev. Lett. **73** (1994) 1529.
10) S. Shin, S. Suga, M. Taniguchi, M. Fujiwara, H. Kanazaki, A. Fujimori, H. Daimon, Y. Ueda, K. Kosuge and S. Kachi: Phys. Rev. B **41** (1990) 4993.
11) S. Vasudevan, M. S. Hegde and C. N. R. Rao: Solid State Commun. **27** (1978) 131.
12) G. A. Sawatzky and D. Post: Phys. Rev. B **20** (1979) 1546.
13) N. Beathman, I. L. Fragala, A. F. Orchard and G. Thornton: J. Chem. Soc. Faraday Trans. 2 **76** (1980) 929.
14) K. E. Smith and V. E. Henrich: Phys. Rev. B **38** (1988) 9224.
15) K. E. Smith and V. E. Henrich: Phys. Rev. B **38** (1988) 9571.
16) S. Shin, Y. Tezuka, T. Kinoshita, A. Kakizaki, T. Ishii, Y. Ueda, W. Jang, H. Takei, Y. Chiba and M. Ishigame: Phys. Rev. B **46** (1992) 9224.
17) S. Shin, Y. Tezuka, T. Kinoshita, T. Ishii, T. Kashiwakura, M. Tkakahashi and Y. Suda: J. Phys. Soc. Jpn. **64** (1995) 1230.
18) M. Abbate, H. Pen, M. T. Czyzyk, F. M. F. de Groot, J. C. Fuggle, Y. J. Ma, C. T. Chen, F. Sette, A. Fujimori, Y. Ueda and K. Kosuge: J. Electron Spectrosc. Relat. Phenom. **62** (1993) 185.
19) X. W. Lin, Y. Y. Wang, V. P. Dravid, P. M. Michalakos and M. C. Kung: Phys. Rev. B **47** (1993) 3477.
20) M. Terauchi, R. Kuzuo, F. Satoh, M. Tanaka, K. Tsuno and J. Ohyama: Microsc. Microanal. Microstruct. **2** (1991) 351.
21) M. Tanaka, M. Terauchi, R. Kuzuo, K. Tsuno, J. Ohyama and Y. Harada: *Proc. 50th Annu. Meet. Electron Microscopy Society of America,* eds. G. W. Beily, J. Bentley and J. A. Small (San Francisco Press, San Francisco, 1992) p. 940.
22) R. F. Egerton: *Electron Energy Loss Spectroscopy in the Electron Microscope* (Plenum Press, New York and London, 1996). 2nd ed., Chap. 4, p.245.
23) M. Terauchi, M. Tanaka, T. Takahashi, H. Katayama-Yoshida, T. Mochiku and K. Kadowaki: Jpn. J. Appl. Phys. **34** (1995) L1524.
24) V. P. Zhuze, A.A. Andreev and A. I. Shelykh: Fiz. Tverd. Tela **10** (1968) 3674. Translation: Sov. Phys.-Solid State **10** (1968) 2914.
25) H. Ehrenreich and H. R. Philipp: Phys. Rev. **128** (1962) 1622.
26) I. Balberg: Phys. Lett. A **43** (1973) 497.
27) J. Zaanen, G. A. Sawatzky, J. Fink, W. Speier and J. C. Fuggle: Phys. Rev. B **32** (1985) 4905.
28) T. Takahashi, F. Maeda, H. Katayama-Yoshida, Y. Okabe, T. Suzuki, A. Fujimori, S. Hosoya, S. Shamoto and M. Sato: Phys. Rev. B **37** (1988) 9788.